

<b>Zeitschrift:</b>	Helvetica Physica Acta
<b>Band:</b>	33 (1960)
<b>Heft:</b>	III
<b>Artikel:</b>	Interactions of K <sup>-</sup> -mesons at rest in nuclear emulsions. VI., The single nucleon capture mode
<b>Autor:</b>	Koch, W. / Eisenberg, Y. / Nikolic, M.
<b>DOI:</b>	<a href="https://doi.org/10.5169/seals-113075">https://doi.org/10.5169/seals-113075</a>

#### **Nutzungsbedingungen**

Die ETH-Bibliothek ist die Anbieterin der digitalisierten Zeitschriften auf E-Periodica. Sie besitzt keine Urheberrechte an den Zeitschriften und ist nicht verantwortlich für deren Inhalte. Die Rechte liegen in der Regel bei den Herausgebern beziehungsweise den externen Rechteinhabern. Das Veröffentlichen von Bildern in Print- und Online-Publikationen sowie auf Social Media-Kanälen oder Webseiten ist nur mit vorheriger Genehmigung der Rechteinhaber erlaubt. [Mehr erfahren](#)

#### **Conditions d'utilisation**

L'ETH Library est le fournisseur des revues numérisées. Elle ne détient aucun droit d'auteur sur les revues et n'est pas responsable de leur contenu. En règle générale, les droits sont détenus par les éditeurs ou les détenteurs de droits externes. La reproduction d'images dans des publications imprimées ou en ligne ainsi que sur des canaux de médias sociaux ou des sites web n'est autorisée qu'avec l'accord préalable des détenteurs des droits. [En savoir plus](#)

#### **Terms of use**

The ETH Library is the provider of the digitised journals. It does not own any copyrights to the journals and is not responsible for their content. The rights usually lie with the publishers or the external rights holders. Publishing images in print and online publications, as well as on social media channels or websites, is only permitted with the prior consent of the rights holders. [Find out more](#)

**Download PDF:** 17.01.2026

**ETH-Bibliothek Zürich, E-Periodica, <https://www.e-periodica.ch>**

## Interactions of $K^-$ -Mesons at Rest in Nuclear Emulsions

### VI. The Single Nucleon Capture Mode

by **W. Koch, Y. Eisenberg\***), **M. Nikolić\*\***), **M. Schneeberger**  
and **H. Winzeler**

Physikalisches Institut der Universität Bern

(19. XI. 1959)

*Abstract.* From an analysis of the pion producing events in  $K^-$ -captures at rest in nuclear emulsion, the features of the single nucleon  $K^-$ -capture mode were studied. Using the pion and  $\Sigma$ -hyperon emission probabilities obtained in the present experiment, and assuming charge independence, all the single nucleon ( $1N$ ) reaction rates could be determined. Comparing our data to other  $K^-$ -absorption experiments, the energy dependence of the  $1N$  matrix elements becomes evident. It is estimated that  $63\% \pm 5\%$  of  $K^-$ -captures lead to a  $1N$  reaction and the rest give rise to multi-nucleon reactions. A study of electrons associated with the  $K^-$ -capture stars indicates that a large fraction of the  $1N$  captures take place in the light emulsion nuclei and that most of the multi-nucleon captures take place in the heavy nuclei. It is also shown that the  $\Sigma$  (or  $\pi$ ) charge exchange scattering is small, in contrast to a large  $\Sigma$ -interaction ( $\Sigma \rightarrow \Lambda$ ) cross section.

#### 1. Introduction

In a previous paper (V) the results concerning the multinucleon (also  $2N$ ) capture mode of  $K^-$ -mesons at rest in nuclear emulsions were presented. In the present work we shall discuss the single nucleon ( $= 1N$ )-capture mode, obtained from a complete analysis of about 1100  $K^-$ -absorptions at rest in emulsions.

From the detailed analysis of all events observed it will be shown that  $63\% \pm 5\%$  of all  $K^-$ -absorptions lead to a  $1N$ -capture. This number does not depend, however, on the complete analysis, and could be obtained (assuming charge independence) from the total number of directly observed pions and from the pion absorption probability, since a  $1N$ -absorption – by definition – has a pion in its final state:  $K^- + N \rightarrow Y + \pi$ . Thus the results given in the present paper will be based upon the study of about 700  $1N$ - $K^-$ -captures.

\*) Also from the Weizmann Institute of Science, Rehovoth.

\*\*) On leave of absence from the Institute of Nuclear Sciences, Boris Kidrich, Belgrade.

A detailed and complete discussion of the raw observed values of all 1100 stars is given in V.

The pion events,  $\pi$ -energy spectra, and the  $\pi^+/\pi^-$  ratio are discussed in section 2 of the present work. In section 3 the emission values of the  $1N-\Sigma$ -hyperon events (namely,  $\Sigma$ -hyperons arising from a  $1N-K^-$ -capture) are briefly summarized. The detailed derivation of the  $\Sigma$ -emission values from the raw observed values, and the separation into  $1N$ - and  $2N-\Sigma$ -events is given in V.

In section 4 the pion and  $\Sigma$ -hyperon absorption probabilities are discussed, and in section 5 the single nucleon reaction rates are presented and compared with the reaction rates obtained in other experiments.

The results of a search for electrons associated with  $1N$ - and  $2N-K^-$ -absorptions are given in section 6, and in section 7 the final conclusions of the present work are summarized.

## 2. The $\pi$ -Events

We have actually observed 373  $\pi$ -mesons and estimated that about 37 pions were lost in the extreme 10% of the emulsions (see V). Thus, the total number of charged pions emitted in all  $K^-$ -captures in the present experiment becomes 410, and the ratio: (charged  $\pi$ 's emitted)/(all  $K^-$ -stars) is  $37.2\% \pm 1.9\%$ , in good agreement with the corresponding value recently published by the  $K^-$ -Collaboration<sup>1</sup>.

The energy spectrum of all the pions observed is given in Figure 1, and that of the positive and negative pions in Figures 2 and 3, respectively. The dimensions of our stack were such that pions above 100 MeV could seldom be stopped and identified. It should not be expected to find positive pions above 95 MeV, since the only production mechanism for  $\pi^+$  is the  $(\pi^+ \Sigma^-)$ -reaction the  $Q$  value of which is 95 MeV. One may expect, however, negative pions above 95 MeV, from the  $(\pi^- \Lambda^0)$ -reaction ( $Q$  value of  $\approx 170$  MeV). The few pions with energies  $> 90$  MeV which we were able to identify (3 events) were negative. No positive pion having an energy above 90 MeV was identified. The corrected number of pions with energies exceeding 95 MeV is 41. 9 of these had kinetic energy certainly (outside one standard deviation) above 120 MeV. This seems to indicate that the  $\Sigma^-$ -capture in negative energy states<sup>2</sup>) and a simultaneous emission of fast  $\pi^+$  ( $> 95$  MeV) from the  $(\pi^+ \Sigma^-)$ -reaction does not play an important role in the  $K^-$ -absorptions at rest in nuclear emulsions, and that most of the fast pions are due to the  $(\pi^- \Lambda^0)$ -reaction.

The total  $(\pi^- \Lambda^0)$ -production rate, however, is expected to exceed the number of 41 events considerably because of the large inelastic scattering cross section of pions in the corresponding energy interval<sup>3</sup>) and also

because  $\approx 1/3$  of the pions from this reaction are produced with energies  $< 95$  MeV.

The unidentified pions (156 of 410) were divided, at each energy interval, according to the proportions of identified pions in the same energy

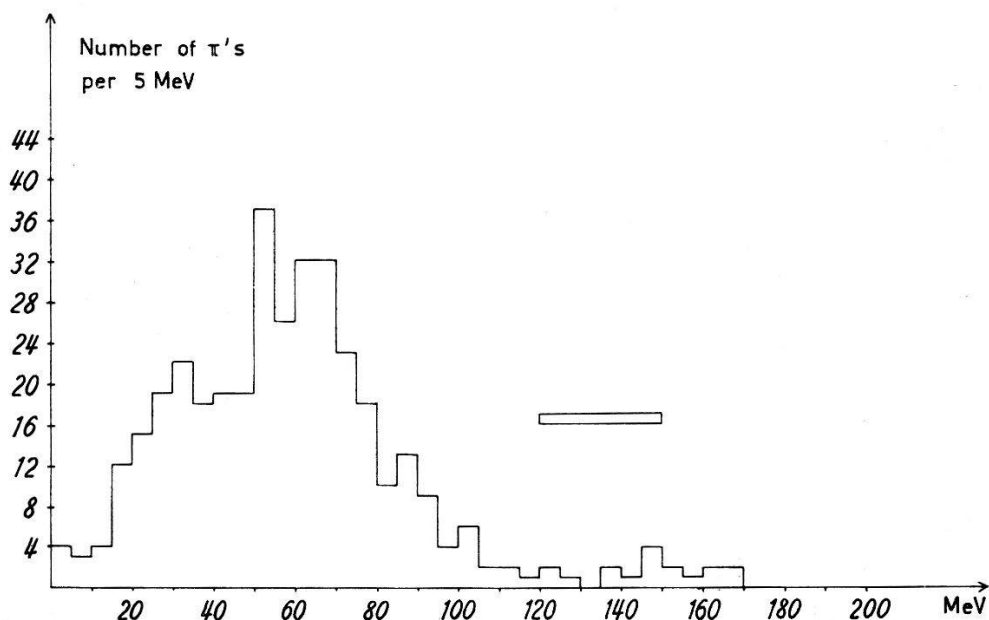


Fig. 1  
Energy spectrum of the 373 observed pions

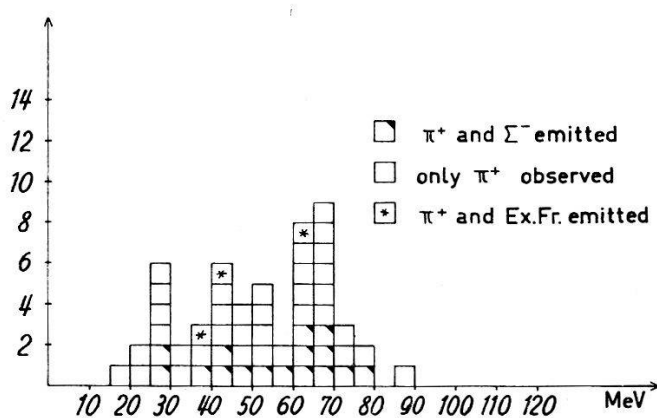


Fig. 2  
Energy spectrum of the 54 identified  $\pi^+$  mesons

interval. Pions having kinetic energy above 95 MeV, were assumed to be all negative and originate from the  $(\pi^- \Lambda^0)$ -reaction.

The final pion emission values which we have obtained are:

positive pions: 80

negative pions: 330

$\pi^+/\pi^-$  ratio =  $0.24 \pm 0.03$

These numbers will be used in section 6, in the derivation of the single nucleon reaction rates. The  $\pi^+/\pi^-$  ratio obtained in this experiment does not agree with the bubble chambers results<sup>4)</sup> extrapolated for  $K^-$ -absorptions at rest in nuclear emulsions (using an  $n/p$  ratio of 1.27). The reason

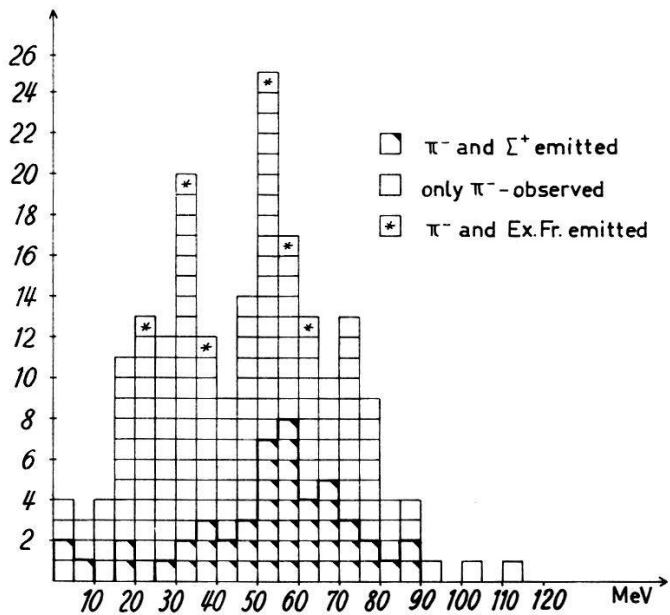


Fig. 3  
Energy spectrum of the 200 identified  $\pi^-$  mesons

for this discrepancy, as was stated before (see III), is the  $K^-$ -nucleon relative momentum dependence of the  $1N$ -matrix elements (due to the nucleon momentum spread in complex nuclei). The  $\pi^+/\pi^-$ -ratio observed in bubble chambers<sup>4)</sup> and emulsions is summarized in Table 1 below. (All numbers extrapolated to emulsions using  $n/p$  ratio of 1.27). The energy dependence of this ratio is quite clear.

Table 1  
 $\pi^+/\pi^-$  ratio in  $K^-$ -absorptions

Experiment	Relative $K^-$ -Nucleon momentum, MeV/c	$\pi^+/\pi^-$ ratio
<i>H</i> -bubble chamber $K^-$ at rest . . . . .	0	0.83
<i>D</i> -bubble chamber (a) $K^-$ at rest . . . . .	70	0.41
Present experiment $K^-$ at rest, emulsions	120	$0.24 \pm 0.03$
<i>H</i> -bubble chamber, $K^-$ at flight . . . . .	420	0.23
Emulsions (b) $K^-$ at flight . . . . .	380	$0.10 \pm 0.04$

(a) The derived proton and neutron absorption rates were used. See section 5.  
(b) Based upon the combined results of III and ref. 5.

### 3. The $\Sigma$ -Hyperon Events

The observed values as well as the derivation of the emission values and the separation into  $1N$  and  $2N$ -events were already given in detail in V. We shall summarize here only the main steps used in the analysis:

(a) Each definitely identified  $\Sigma^-$  at rest (namely, each baryon coming to rest and producing a two or more prong star, or a star with only one prong longer than  $200 \mu$ ) was assumed to be equivalent to 2.6  $\Sigma^-$ -hyperons emitted. This  $\Sigma^-$ -prong correction factor was obtained by using world statistics of  $K^-$ -absorption on free protons in nuclear plates.

(b) The slow (below 50 MeV) unidentified  $\Sigma^\pm$ -hyperons (6 events) were divided by arguments concerning the  $\Sigma$ -life time and the energy spectrum.

(c) A small tail (5 events) of  $2N-\Sigma$ 's was assumed to be among the slow  $1N-\Sigma$ 's.

Using these corrections (see V) the following  $1N$ -emission values were obtained:

Table 2  
Corrected  $1N-\Sigma$ -hyperon emission values

Type of event	Numbers emitted
$(\Sigma^- + \pi^+)$ . . . . .	39
$(\Sigma^- + 0 \pi)$ . . . . .	46
All $\Sigma^-$ . . . . .	85
$(\Sigma^+ + \pi^-)$ . . . . .	54
$(\Sigma^+ + 0 \pi)$ . . . . .	10
All $\Sigma^+$ . . . . .	64
All $1N-\Sigma$ -hyperons . . .	149

### 4. The Pion and $\Sigma$ -Hyperon Emission Probabilities

The pion and  $\Sigma$ -hyperon experimental emission probabilities which have been used before (see III and IV), namely:

$$E_{\pi^-}^{(\Sigma)} = \frac{N(\pi^-, \Sigma^+)_{em}}{N(\Sigma^+)_{em}} \quad (1)$$

$$E_{\Sigma^-} = \frac{N(\pi^+, \Sigma^-)_{em}}{N(\pi^+)_{em}}$$

could be somewhat biased since the production directions of the pion and hyperon are correlated (see Figures 4 and 5 below), and peaked at large angles. Thus, an observed  $\Sigma^+$ -hyperon (or  $\pi^+$ -meson) could be preferentially due to an emission direction away from the center of the nucleus, and its  $\pi^-$  (or  $\Sigma^-$ ) partner would be travelling in the direction of a large nucleon density which would result in a stronger absorption. One has to

correct, therefore, for the above correlation. The correction will depend somewhat on the model assumed for the  $K^-$ -capture, but since it is small anyhow, the corrected emission probabilities will not be very sensitive to the model assumed.

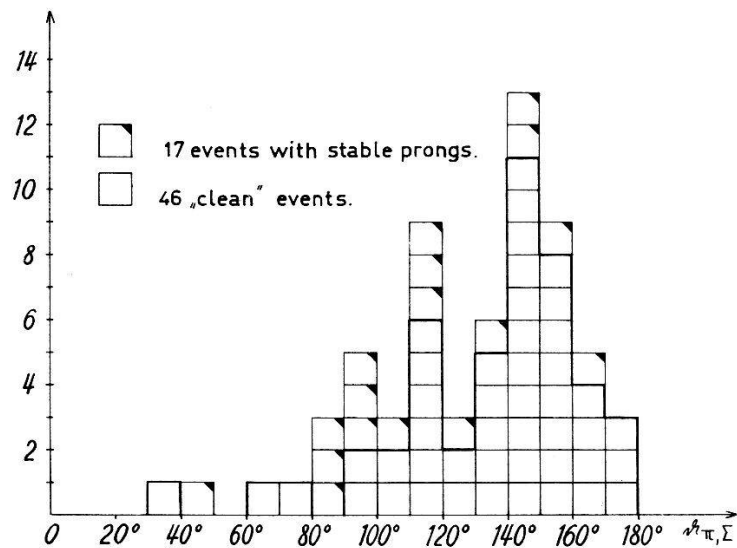


Fig. 4  
Distribution of angles between  $\pi$ - and  $\Sigma$ -emission directions in  $(\pi, \Sigma)$  events

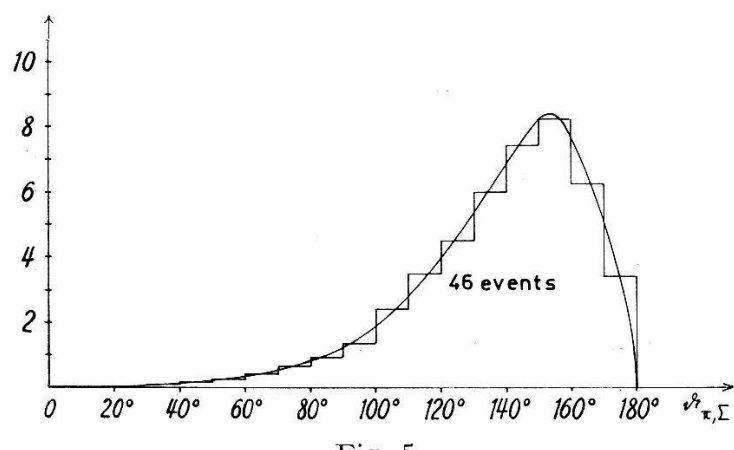


Fig. 5  
Distribution of angles between  $\pi$ - and  $\Sigma$ -emission directions in  $(\pi, \Sigma)$  events,  
calculated from a nucleon momentum distribution  
 $\sim p^2 e^{-p^2/a^2}$  ( $a = 170$  MeV/c), assuming the  $1/v_{\text{rel}}$ -law.

Since one needs here the use of a distinct model we shall take for these considerations the peripheral model, but we must emphasize that this does not mean that we commit ourselves with this assumption. It only means that a peripheral model would be in good agreement with the results or e. g. angular distribution in  $(\pi, \Sigma)$ -events, the distribution of  $(T_\pi + T_\Sigma)$  (Figure 6) the large percentage of clean  $(\pi, \Sigma)$ -events and the small values of  $A_\pi$ .

We shall thus assume a peripheral absorption in the calculation of the  $\pi^-$ - and  $\Sigma$ -emission probability. As was stated before, the results will not be sensitive to this assumption.

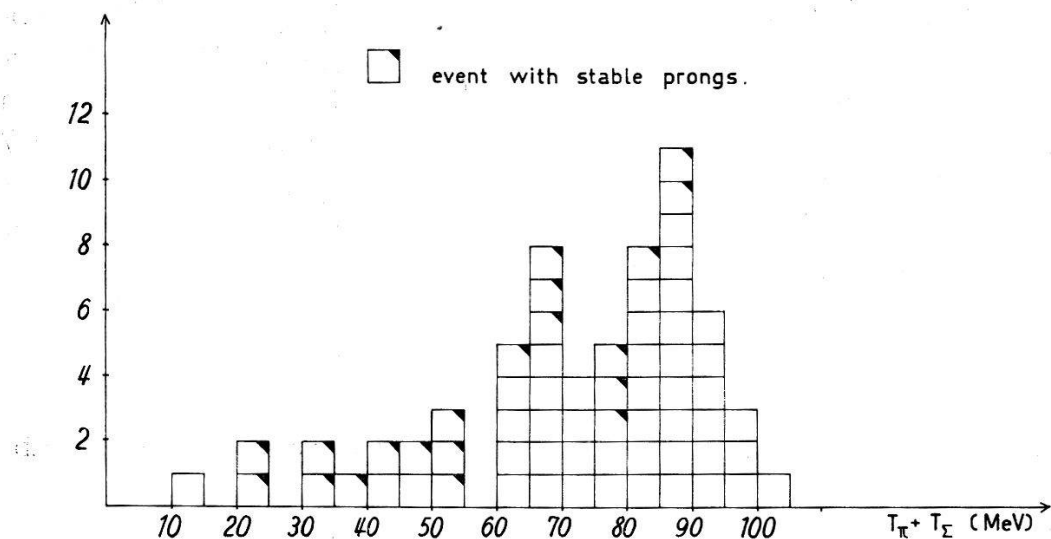


Fig. 6  
Distribution of  $(T_{\pi} + T_{\Sigma})$  obtained from 64  $(\pi, \Sigma)$ -events

In general, for any capture model, the relation between the experimentally observed emission probability  $E_a^*$  of particle a and the correct emission of particle b ( $E_b$ ) is given by:

$$E_a^* = \frac{E_{a,b}}{E_b} \quad (2)$$

This is identical to relation (1) above. Here  $E_{a,b}$  is the probability for simultaneous emission of particles a, b. The relation between  $E_{a,b}$  and  $E_a$  and  $E_b$  is more complicated and will depend upon the model assumed. This is given in detail in the appendix. We are thus able to calculate from our experimental values the corrected  $\pi^-$ - and  $\Sigma^-$ -emission probabilities. But we can also determine directly  $E_{\Sigma^+}$  (see appendix) from

Table 3  
Emission probabilities

Particle	Corrected emission probabilities
$\pi^+$ in associated $(\pi, \Sigma)$ production . . .	$E_{\pi^+}^{(\Sigma)} = 0.91 \pm 0.05$
$\pi^-$ in associated $(\pi^-, \Lambda^0)$ production . . .	$E_{\pi^-}^{(\Lambda)} = 0.8 \pm 0.1$
$1N-\Sigma^+$ -hyperon . . . . .	$E_{\Sigma^+} = 0.52 \pm 0.06$
$1N-\Sigma^-$ -hyperon . . . . .	$E_{\Sigma^-} = 0.43 \pm 0.05$
simultaneous $\Sigma^+$ and $\pi^-$ emission . . .	$E_{\pi^-, \Sigma^+} = 0.44$
simultaneous $\Sigma^-$ and $\pi^+$ emission . . .	$E_{\pi^+, \Sigma^-} = 0.36$

a detailed study of the fast protons (above 30 MeV) associated with the  $\pi$ -events. The final emission values, given in Table 2 below, were obtained by requiring best agreement with our observational values. We had no way of determining directly from our experiment  $E_{\pi^-}^{(A)}$  (the emission probability of the  $\pi^-$  associated with a direct  $\pi^- A^0$ -production). It is expected to be smaller than  $E_{\pi}^{(\Sigma)}$ , since the pion interaction cross-section rises in this energy range. By using  $\pi^-$ -interaction data and figure 7 (appendix) we get:  $E_{\pi}^{(A)} = 0.8 \pm 0.1$ . This value, together with the other emission probabilities in Table 3 will be used in the next section for determining all the  $1N$ -reaction rates.

### 5. The Single Nucleon Reaction Rates

The following are the seven possible reactions resulting from  $K^-$ -absorptions on single nucleons:

	Reaction	Reaction rate
(1)	$K^- + p \rightarrow \pi^+ + \Sigma^-$	$r^2 + 2/3 + 2 \sqrt{2/3} r \cos \varphi$
(2)	$\rightarrow \pi^- + \Sigma^+$	$r^2 + 2/3 - 2 \sqrt{2/3} r \cos \varphi$
(3)	$\rightarrow \pi^0 + \Sigma^0$	$2/3$
(4)	$\rightarrow \pi^0 + \Delta^0$	$2 r_A^2$
(5)	$K^- + n \rightarrow \pi^0 + \Sigma^-$	$2 r^2$
(6)	$\rightarrow \pi^- + \Sigma^0$	$2 r^2$
(7)	$\rightarrow \pi^- + \Delta^0$	$4 r_A^2$

The reaction rates were obtained for a self-conjugate nucleus (number of neutrons equals number of protons) by assuming charge independence (see III for details). For comparison with actual emulsion experiments, the neutron reactions should be multiplied by 1.27 (the average  $n/p$  ratio in emulsions, assuming a modified Fermi-Teller  $Z$  capture law<sup>6</sup>), which yields 30% captures in CNO and 70% in AgBr). The matrix elements (see III) are:

$$r \cdot e^{i\varphi} = \frac{\langle T = 1 | H_{\Sigma} | T = 1 \rangle}{\langle T = 0 | H_{\Sigma} | T = 0 \rangle}, \quad |r_A| = \left| \frac{\langle T = 1 | H_A | T = 1 \rangle}{\langle T = 0 | H_A | T = 0 \rangle} \right|$$

From the pion and  $\Sigma$ -hyperon emission values (sections 2 and 3 respectively) and by using the emission probabilities given in section 4, we can derive all the single nucleon production values, assuming charge independence. The method has been discussed before in detail in IV. We shall, therefore, mention it very briefly here. Let  $N( )_{\text{em}}$  be the emission values of the particles in the brackets, and let  $N( )_{\text{prod}}$  be the production values of the bracketed particles. Then, from the result of section 4 we get:

$$N(\pi^+ \Sigma^-)_{\text{prod}} = \frac{N(\pi^+)_{\text{em}}}{E_{\pi^+}^{(\Sigma)}} \quad (1)$$

$$N(\pi^- \Sigma^+)_{\text{prod}} = \frac{N_2(\pi^- \Sigma^+)_{\text{em}}}{E_{\pi^- \Sigma^+}} \quad (2)$$

$$N(\pi^0 \Sigma^-)_{\text{prod}} = \frac{1}{E_{\Sigma^-}} \{ N(0 \pi, \Sigma^-)_{\text{em}} - [E_{\Sigma} - E_{\Sigma^- \pi^+}] N(\pi^+ \Sigma^-)_{\text{prod}} \} \quad (5)$$

$$N(\pi^- \Sigma^0)_{\text{prod}} = N(\pi^0 \Sigma^-)_{\text{prod}}, \text{ by charge independence} \quad (6)$$

$$N(\pi^- \Lambda^0)_{\text{prod}} = \frac{1}{E_{\pi^-}^{(\Lambda)}} \{ N(\pi^-)_{\text{em}} - E_{\pi^-}^{(\Sigma)} [N(\pi^- \Sigma^+)_{\text{prod}} + N(\pi^- \Sigma^0)_{\text{prod}}] \} \quad (7)$$

and again by charge independence:

$$N(\pi^0 \Sigma^0)_{\text{prod}} = \frac{1}{2} [N(\pi^+ \Sigma^-)_{\text{prod}} + N(\pi^- \Sigma^+)_{\text{prod}} - \frac{1}{1.27} N(\pi^0 \Sigma^-)_{\text{prod}}] \quad (3)$$

$$N(\pi^0 \Lambda^0)_{\text{prod}} = \frac{1}{2.54} N(\pi^- \Lambda^0)_{\text{prod}}. \quad (4)$$

The final reaction rates obtained in this experiment are summarized in Table 4 below. They are in fair agreement with the results of the  $K^-$ -Collaboration<sup>1</sup>). The errors quoted are statistical as well as systematic,

Table 4

Reaction	Production values	
	Numbers	Percentages
(1) $\pi^+ \Sigma^-$ . . . .	$88 \pm 12$	$12.6 \pm 1.7$
(2) $\pi^- \Sigma^+$ . . . .	$123 \pm 26$	$17.7 \pm 3.6$
(3) $\pi^0 \Sigma^0$ . . . .	$68 \pm 17$	$9.7 \pm 2.4$
(4) $\pi^0 \Lambda^0$ . . . .	$65 \pm 22$	$9.3 \pm 3.1$
(5) $\pi^0 \Sigma^-$ . . . .	$95 \pm 30$	$13.6 \pm 4.3$
(6) $\pi^- \Sigma^0$	$95 \pm 30$	$13.6 \pm 4.3$
(7) $\pi^- \Lambda^0$ . . . .	$164 \pm 56$	$23.5 \pm 8.0$
All . . . . .	$698 \pm 52$	100%

matic, coming mostly from uncertainties in the emission probabilities and the  $\Sigma^-$ -correction factor (section 3).

The relative number of single nucleon captures in  $K^-$ -absorptions at rest in nuclear emulsions is then:  $(698 \pm 52)/1104 = 63\% \pm 4.5\%$ . This number is in agreement with the recently published number ( $\sim 30\%$  2N-capture) by the  $K^-$ -Collaboration (Kiev reports, 1959). We wish to emphasize that this number is not sensitive to the ratio of heavy to light nuclei capture assumed. The error in the total number of 1N-captures is essentially determined by the statistical error in the number of observed pions ( $\sim 400$  events) and by the systematic error in the pion absorption probabilities. But since the pion absorption probability is any-

how small, the total number of  $1N$ -captures is not very sensitive to it. Also, one should note that the errors of the individual reaction rates are correlated (see method of derivation of the reaction rates outlined above).

Recently<sup>4)</sup>, the absorption of  $K^-$  at rest in deuterium and the  $K^-p$  interaction at flight has been studied by the Berkeley Bubble Chamber Groups. All the published single nucleon reaction rates for the various experiments are given in Table 5. The single nucleon reaction rates in deuterium were derived\*) from the data published by the  $D$ -Bubble Chamber-Group<sup>4)</sup> by assuming charge independence and by taking into account only  $\Sigma \rightarrow \Lambda$ -transition. The  $\Sigma$ -charge exchange probability is probably small\*) and was neglected. By studying Table 5 it becomes clear, as was pointed out in III, that the  $K^-$ -nucleon interaction depends rather strongly upon the relative  $K^-$ -N-momentum. In particular, the large change in  $\cos\varphi$  (the phase angle between the  $T = 1$  and  $T = 0$  matrix elements) between  $\bar{P}_{\text{rel}} = 0$  and  $\bar{P}_{\text{rel}} = 70$  MeV/c is apparent. Later on,  $\varphi$  does not seem to depend anymore upon the energy. On the other hand, with the increase of  $\bar{P}_{\text{rel}}$ , the  $T = 1$  state, both for the  $\Sigma$  and  $\Lambda$ -reactions, seems to become more and more dominant. Thus also neutron captures seem to become more important at high  $\bar{P}_{\text{rel}}$  values than at lower ones. The increase in direct  $\Lambda$ -production is opposite to what one would expect from simple phase-space arguments. The normalizing momentum phase-space factor  $(\bar{P}_{\Sigma}^{\text{CM}}/\bar{P}_{\Lambda}^{\text{CM}})^2$  varies only from  $\sim 0.5$  to  $\sim 0.6$  in the energy range considered here. Thus the  $\Sigma$ - and  $\Lambda$ -reactions seem to depend differently upon  $\bar{P}_{\text{rel}}$ .

## 6. The Relative Yield of $1N$ and $2N$ Reactions in $K^-$ Captures in Heavy and Light Nuclei

A systematic search was conducted for electrons associated with  $K^-$ -absorptions giving rise to  $\pi$ -mesons and slow  $\Sigma$ -hyperons and to fast (over 50 MeV)  $\Sigma$ -hyperons and fast (over 60 MeV) protons. The first class of events represents certain  $1N$ -absorptions and the second class certain  $2N$ -absorptions. The results of this search are summarized in Table 6.

A certain electron had to have over 4 grains (15 keV). Questionable electrons are followed by a questionmark. The final yield was obtained by taking into account half the questionable electrons and by correcting for random background electrons the yield of which was determined from proton endings.

From Table 6 it becomes clear that the yield of electrons is significantly larger in certain  $2N$ -absorptions than in certain  $1N$ -absorptions. Also,

\*) Y. EISENBERG and D. KESSLER, private communication.

Table 5

Comparison of the single nucleon reaction rates for a self-conjugate nucleus  
(number of protons equals to the number of neutrons)

Reaction	$H$ -bubble chamber $K^-$ at rest $\bar{P}_{\text{rel}} = 0$	Observed Rates in Percentages			
		$D$ -bubble chamber $K^-$ at rest $\bar{P}_{\text{rel}} \approx 70 \text{ MeV/c}$	$K^-$ at rest, emuls. $\bar{P}_{\text{rel}} \approx 120 \text{ MeV/c}$	Bern results (III) $K^-$ at flight $\bar{P}_{\text{rel}} \approx 380 \text{ MeV/c}$	$H$ -bubble chamber $K^-$ at flight $\bar{P}_{\text{rel}} \approx 420 \text{ MeV/c}$
$K^- p \rightarrow \pi^+ \Sigma^-$	32.6	20.8	14.1	9.6	14.2
$\pi^- \Sigma^+$	15.2	28.7	19.8	14.2	15.8
$\pi^0 \Sigma^0$	19.6	21.0	10.9	4.7	9.1
$\pi^0 \Lambda^0$	5.1	4.9	10.3	14.3	12.4
$K^- n \rightarrow \pi^0 \Sigma^-$	8.7	7.4	12.1	14.3	11.8
$\pi^- \Sigma^0$	8.7	7.4	12.1	14.3	11.8
$\pi^- \Lambda^0$	10.1	9.8	20.7	28.6	24.9
Numbers of events studied	large. errors are $\sim 2\%$	1650	1100	415	120
$r^2$	0.15	0.12	0.37	1	0.43
$r_A^2$	0.086	0.08	0.32	1	0.45
$\cos \varphi$	0.47	-0.22	-0.18	-0.2	-0.054
$\varphi$	62°	103°	100°	102°	93°
Direct $\Sigma$ prod.	84.8%	85.3%	69%	57%	62.7%
Direct $\Lambda$ prod.	15.2%	14.7%	31%	43%	37.3%

Table 6  
Electrons associated with  $K^-$ -capture stars

Type of event	No. of events	Observed Number of					I + II + + $\frac{1}{2}$ (III + IV)	Yield in %	
		I Blob + $\epsilon$	II $\epsilon$	III Blob + $\epsilon$ (?)	IV $\epsilon$ (?)	V Blob			
( $\pi, \Sigma$ )	65	2	3	2	3	7	7.5	6	9.4% $\pm$ 3.8%
Certain 1N	411	33	32	19	21	56	85	75	18.2% $\pm$ 2.1%
Certain 2N	151	14	24	8	10	16	47	43.4	28.7% $\pm$ 4.4%

when both  $\pi$  and  $\Sigma$  are emitted ( $(\pi, \Sigma)$ -events) the yield seems to be particularly low. Since one expects to find more electrons (both Auger electrons and any others too) associated with  $K^-$ -captures in the heavy emulsion nuclei than with captures in the light nuclei, the above observation indicates quite strongly that captures in AgBr lead more often to a multi-nucleon reaction than  $K^-$ -capture in CNO. For a more quantitative statement one needs to know the proportion of  $K^-$ -captures in CNO and AgBr, and also the yield of electrons upon capture in the various elements. This, unfortunately, is not very well known. If one makes the extreme assumption (which is perhaps not so bad) that  $K^-$ -capture in CNO does not yield any electron emission, we have carried out the analysis for the two possible capture mechanisms: heavy/light absorption ratio is 7/3 (Fermi-Teller Z-law<sup>6</sup>), and heavy/light = 1:1. The results of this analysis are given in Table 7. It seems, for both assumptions, that

Table 7  
1N and 2N absorption yield in light and heavy nuclei

Assumed $K^-$ -capture ratio, heavy/light =	7:3	1:1	
Then: of all 1N reactions . . . . .	58%	41%	in heavy elem.
of all 2N reactions . . . . .	91%	65%	in heavy elem.
Or: in heavy elements . . . . .	48%	48%	2N reactions
in light elements . . . . .	11%	26%	2N reactions

the 2N-capture occurs mostly in the heavy emulsion nuclei. It should be emphasized that the above yield of the 2N-reaction in AgBr is only a lower limit. If the yield of electrons from the light elements is different from zero, using our experimental values, we obtain that more of the 2N-reactions take place in the heavier elements and less in the light elements. The recent data<sup>4)</sup> of the Deuterium bubble chamber group also indicate that the 2N-reaction yield in  $K^-$ -captures in  $D$  is very small.

### 7. Conclusions

We would like to summarize now, briefly, the main conclusions reached in the present works.

(1) The single nucleon  $K^-$ -captures form  $63\% \pm 5\%$  of all  $K^-$ -absorptions at rest in nuclear emulsions. The multi-nucleon  $K^-$ -capture mode forms then  $37\% \pm 5\%$  of all  $K^-$ -absorptions. No evidence of a substantial  $2N$ -capture mode was found in the interactions of fast  $K^-$ -mesons in nuclear emulsions (III, 14).

(2) The single nucleon  $K^-$ -capture matrix elements are energy dependent (see Table 5 section 6). In particular, if the relative C. M.  $K^-$ -nucleon momentum increases, we get that:

- (i) The direct  $\Lambda^0$ -production increases (see section 6 and 3).
- (ii) The  $T = 1$  state  $K^-$ -captures become relatively more and more important, and therefore the neutron to proton  $K^-$ -absorption ratio increases.
- (iii) As soon as  $\bar{P}_{\text{rel}}$  is different from zero, the phase angle between the  $T = 1$  and  $T = 0$  matrix elements changes rapidly. At higher  $\bar{P}_{\text{rel}}$  values, it does not seem to change any more. It might be due to the fact that for  $\bar{P}_{\text{rel}} = 0$ , only pure  $S$  - wave captures take place<sup>10</sup>).

(3) An examination of slow electrons associated with certain  $1N-K^-$ -captures and certain  $2N-K^-$ -captures indicates quite strongly that the  $2N$ -processes occur mostly in the heavy elements of the nuclear emulsion. It seems also (but statistically less significant) that events with associated  $\pi + \Sigma$ -emission occur mostly in the light emulsion elements.

(4) Generally speaking, our single nucleon  $K^-$ -captures data seem to be in agreement with the assumption of peripheral absorptions, but do not exclude the possibility of other capture models. Peripheral absorption is expected from a detailed calculation of a  $K^-$ -cascade in emulsion atoms<sup>77</sup> (taking into account the nuclear matter distribution), and is in agreement with our observations of a very small pion absorption probability, a large correlation both in energy and angle between the pion and  $\Sigma$ -hyperon in the associated  $(\pi, \Sigma)$  events.

(5) Within the framework of our model the  $\pi$ -absorption probability agrees with the pion interaction data (8. 9). The  $\Sigma$ -hyperon absorption probability is much larger, which indicates a very small  $\Sigma$ -interaction ( $\Sigma \rightarrow \Lambda$ ) mean free path in nuclear matter. This statement becomes even stronger if one considers points (3) and (4) above.

(6) The  $\Sigma$  and  $\pi$ -charge exchange scattering is small. Only one probable event of a  $\Sigma$  (or  $\pi$ ) charge exchange scattering inside the nucleus in which the particles were produced, was found. (This is the only published event of that type.)

Our sincere thanks are due to Drs. LOFGREN, JAUNEAU and TEUCHER who exposed the stack for us at the Bevatron. We are especially indebted to Profs. F. G. HOUTERMANS and CH. PEYROU for their continuous interest and many helpful discussions during all the phases of the work. Furthermore we got an interesting suggestion from Dr. E. MARQUIT.

The scanning team did efficient work. We are grateful to Mrs. B. ALBRECHT, E. BLASER, B. DZIUMBLA, E. KOCH, CH. PLUMETTAZ, I. RITSCHARD and S. SCHILT. Mrs. B. ALBRECHT, CH. PLUMETTAZ and I. RITSCHARD made precise measurements for us.

Our further thanks are due to the Schweizerische Studienkommission für Atomenergie, to the Kommission für Atomwissenschaften and to the Schweizer Nationalfonds for financial support of this work.

## APPENDIX

### A. Combined Emission Probabilities

When two particles  $a$  and  $b$  are produced inside the nucleus an approximate emission probability  $E_a^*$  for particle  $a$  is given by the number of events, where  $a$  and  $b$  were emitted  $N(a, b)_{\text{em}}$  and the number of events where  $a$  was absorbed and only  $b$  was emitted  $N(0a, b)_{\text{em}}$ .

$$E_a^* = \frac{N(a, b)_{\text{em}}}{N(a, b)_{\text{em}} + N(0a, b)_{\text{em}}} = \frac{E_{a,b}}{E_b} \quad (1)$$

We shall calculate now the correction which has to be applied to  $E_a^*$  in order to get the true emission probability  $E_a$ , defined by:

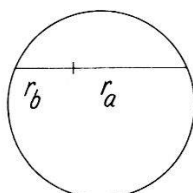
$$E_a = \frac{N(a)_{\text{emitted}}}{N(a)_{\text{produced}}} \quad (2)$$

$E_a^*$  is different from  $E_a$  when the emission directions of  $a$  and  $b$  are correlated. The relation between  $E_a^*$  and  $E_a$  will depend upon the angular correlation between  $a$  and  $b$ , and upon the production position in the nucleus. The calculation will be carried out for particles emitted in opposite directions under two assumptions: (a) homogeneous production throughout the entire nuclear volume, and (b) surface production.

Each emission probability can be written as a product of two factors,  $e$  and  $T$ .  $e$  is the emission probability for a nucleus having no potential barrier (depending only on the mean free path  $\lambda$  in nuclear matter, and  $T$  is the probability for the surface transmission (see also ref. 11).

For the homogeneous production we have:

$$e_{a,b}^{\text{hom}} = \iint_{\text{Volume}} e^{-\frac{r_a}{\lambda_a}} e^{-\frac{r_b}{\lambda_b}} dV$$



or, after integration:

$$e_{a,b}^{\text{hom}} = \frac{3}{\Delta_a - \Delta_b} \left\{ \frac{1}{\Delta_b^2} [1 - (1 + \Delta_b) e^{-\Delta_b}] \frac{1}{\Delta_a^2} [1 - (1 + \Delta_a) e^{-\Delta_a}] \right\} \quad (3)$$

where  $\Delta_a = 2R/\lambda_a$ ,  $\Delta_b = 2R/\lambda_b$  and  $R$  is the nuclear radius. Note that for the limiting case  $\Delta_b \rightarrow 0$ , we get CAPP's<sup>11)</sup> formula:

$$e^{\text{hom}} = \frac{3}{\Delta^3} \left[ \frac{1}{2} \Delta^2 + (1 + \Delta) e^{-\Delta} - 1 \right]. \quad (4)$$

$e^{\text{hom}}$  as a function of  $\Delta$  is plotted in Figure 7.  $e_{a,b}$  can be written, by using (4), as a function of  $e_a$  and  $e_b$ . Since we have:

$$E = e \cdot T, \quad \text{and} \quad E_{a,b} = T_a \cdot T_b \cdot e_{a,b} \quad (5)$$

the true  $E_a$  can now be calculated from the experimental  $E_a^*$  (see (1) above) if  $E_b$ ,  $T_a$  and  $T_b$  are known. If only  $E_a^*$  and  $E_b^*$  are known then by successive iterations (knowing  $T_a$  and  $T_b$ )  $E_a$  and  $E_b$  can be calculated.

For the surface model we have:

$$e^{\text{sur.}} = 1/2 + 1/2 \Delta (1 - e^{-\Delta}). \quad (6)$$

$e^{\text{sur.}}$  as a function of  $\Delta$  is also plotted in Figure 7. In this case one gets immediately:

$$e_{a,b}^{\text{sur.}} = e_a^{\text{sur.}} + e_b^{\text{sur.}} - 1, \quad (7)$$

and by (1) we obtain:

$$e_a^{\text{sur.}} = 1 - e_b (1 - e_a^*). \quad (8)$$

Note that due to the linearity of (7), these relations are also valid for any mixture of nuclei, namely we always have:

$$\bar{e}_{a,b}^{\text{sur.}} = \bar{e}_a^{\text{sur.}} + \bar{e}_b^{\text{sur.}} - 1. \quad (7')$$

The emission probabilities for particles produced at different distances  $r = aR$  from the center of the nucleus have been calculated for  $a = 0.6$ ; 0.8; 0.9 and 1 ( $\equiv$  surface model) as functions of  $\Delta$  and are plotted in Figure 7. In the case  $a = r/R = 0.8$  the emission probabilities are at least for small  $\Delta$  the same as in the case of the homogeneous model.

In the present experiment, due to the relatively high energy of the pions produced, we have assumed.  $T_{\pi^+} = T_{\pi^-} = 1$ . For the  $\Sigma$ -hyperons, using Capp's internal production spectrum<sup>11)</sup>, a  $\Sigma$ -nuclear potential of  $-10$  MeV, and a Coulomb potential of  $\pm 9$  MeV for the heavy emulsion nuclei and  $\pm 3$  MeV for the light emulsion nuclei, we get (classically):

$$T_{\Sigma^+} = T_{\Sigma^0} = 0.86, \quad T_{\Sigma^-} = 0.68. \quad (9)$$

From (1), (7), (8) and (9) one can, in principle, calculate the individual  $\pi$  and  $\Sigma$ -emission probability as well as the combined emission probability  $E_{\pi, \Sigma}$ .

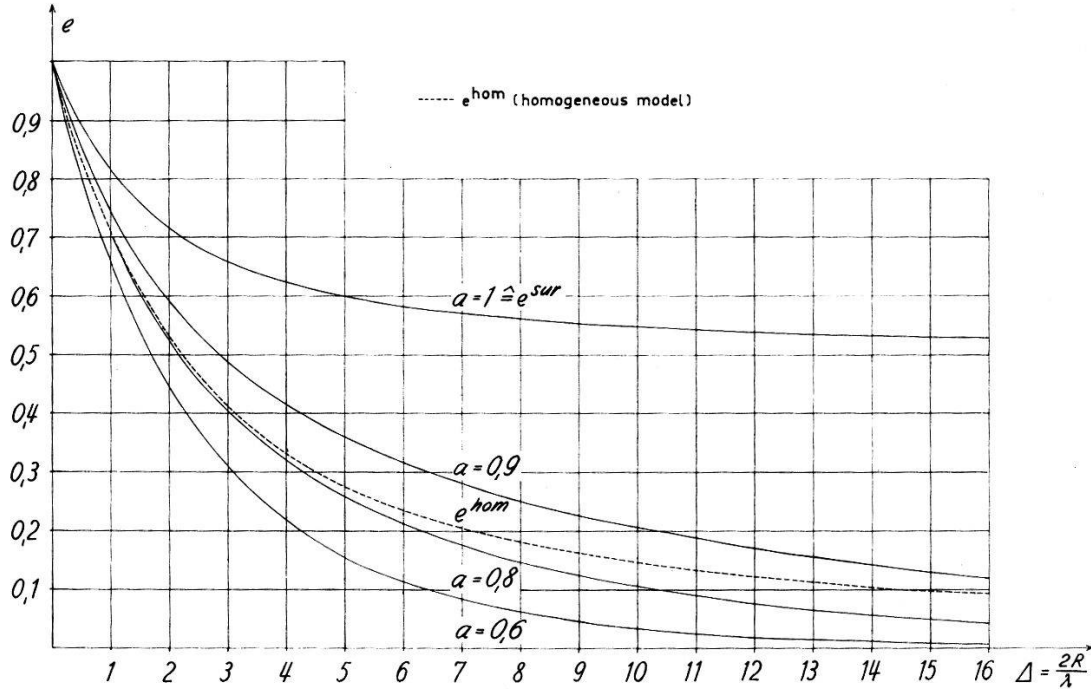


Fig. 7

Emission probabilities in dependence of  $A = 2R/\lambda$  for particles produced at different distances  $r = aR$  from the center of the nucleus

### B. The $\pi$ and $\Sigma$ emission probabilities

The  $\Sigma^-$ -emission probability is obtained directly from our experimental values (see section 2):

$$E^* = \frac{N(\pi^+, \Sigma^-)_{\text{em}}}{N(\pi^+, \Sigma^-)_{\text{em}} + N(\pi^+, 0\Sigma)} = \frac{39}{80} = 0.49 \pm 0.14 \quad (1)$$

Similarly, the emission probability of  $\pi^-$ -mesons associated with  $\Sigma$ -production is:  $E_{\pi^-}^{(\Sigma)*} = 54/64 = 0.85 \pm 0.1$ . With the help of part A above, one gets for the corrected emission probabilities:

$$E_{\Sigma^-} = 0.50, \quad E_{\pi^-}^{(\Sigma)} = 0.89. \quad (2)$$

From this value of  $E_{\Sigma^-}$ , using the results of A above and the neutron/proton ratio in emulsions, one can calculate  $E_{\Sigma^+}$  and  $E_{\Sigma^0}$ . We thus get:

$$E_{\Sigma^+} = 0.61 \pm 0.17. \quad (3)$$

However,  $E_{\Sigma^+}$  could also be determined from the analysis of fast protons associated with  $(\pi^-, 0\Sigma)$  events. This will be demonstrated now.

By comparing the fast ( $> 30$  MeV) proton yield in  $(\pi^+, 0\Sigma)$  and  $(\pi^-, 0\Sigma)$  events (see Table 1 of V), it becomes clear that the  $\Sigma^-$ -absorp-

tions are seldom associated with the emission of fast protons, in contrast to  $\Sigma^+$  and  $\Sigma^\circ$ -absorptions. This is expected, since only neutral particles are produced in  $\Sigma^-$ -captures. The total number of fast ( $> 30$  MeV) protons observed in our entire (corrected) sample of  $(\pi^-, 0 \Sigma)$  events was 79. From this number one has to subtract the contribution of fast ( $> 30$  MeV) protons from: (1) inelastic scattering of  $\pi^-$  (or  $\Lambda^\circ$ ) produced in the  $(\pi^- \Lambda^\circ)$ -reaction, (2) decays of cryptofragments (inseparable hyperfragments). The fast ( $> 30$  MeV) proton yield in the inelastic scattering of  $\pi^-$  (having similar energy as the  $\pi^-$ 's from the  $(\pi^- \Lambda^\circ)$ -reaction) is small—about 10%<sup>12</sup>. Thus we may use our a-posteriori knowledge of the  $(\pi^- \Lambda^\circ)$ -production value ( $\approx 160$  events) for estimating the contribution to fast protons from (1) above. This contribution will not depend strongly upon the exact  $K^-$ -capture model, since the inelastic scattering cross section (in our energy range) is about geometric<sup>3</sup>), and since in the surface model, whenever the pion escapes without going through nuclear matter, the  $\Lambda^\circ$  will go through the nucleus and could also produce fast knock-on protons. Thus, process (1) will give about 16 fast ( $> 30$  MeV) protons associated with  $(\pi^-, 0 \Sigma)$  events. Process (2) above (crypto-fragment decays) contributes very little to the fast proton formation, and can be roughly estimated by the following arguments: The direct and indirect ( $\Sigma + N \rightarrow \Lambda^\circ + N$ ) energy spectra are very similar (see III). Thus, the cryptofragment formation yield per  $\Lambda^\circ$  traversing the nucleus is expected to be the same in both cases. Since the  $\Sigma$ -absorption probabilities are about 0.5, and since also about 50% of the  $\Lambda$ 's (in the surface model) go through the nucleus, the cryptofragment yield per observed pion is roughly constant. Thus we may use our  $(\pi^+, 0 \Sigma)$  events for getting the number of fast ( $> 30$  MeV) protons arising from process (2). Since the  $(\pi^+, 0 \Sigma)$  events are very seldom associated with fast protons, we estimate that process (2) would yield about 5 fast ( $> 30$  MeV) protons in our entire 276  $(\pi^-, 0 \Sigma)$  events. The rest—namely  $79 - 16 - 8 = 55$  events—originate then from  $\Sigma^+$  and  $\Sigma_p^\circ$ -absorption. The total number of  $\Sigma^+$ - and  $\Sigma_p^\circ$ -absorptions was determined by extrapolating the energy spectrum of the fast ( $> 30$  MeV) protons in the  $(\pi^-, 0 \Sigma)$  events to zero energy. We thus get  $88 \pm 18$   $\Sigma^+$  and  $\Sigma_p^\circ$ -absorptions. Assuming that the fast proton yield in  $\Sigma^\circ$ -captures is 1/2 that of  $\Sigma^+$ -captures, we get:

$$88 = (E_{\pi^-} - E_{\pi^-, \Sigma^+}) N(\pi^- \Sigma^+)_{\text{prod}} + 1/2 (E_{\pi^-} - E_{\pi^-, \Sigma^\circ}) N(\pi^- \Sigma^\circ)_{\text{prod}} \quad (4)$$

Since the production values depend upon  $E_{\Sigma^+}$  and the experimentally observed values, equation (4) can be solved for  $E_{\Sigma^+}$ , namely:  $E_{\Sigma^+} = 0.52 \pm 0.06$ . With the resulting  $e_{\Sigma^+}$  the experimental value  $E_{\pi^-}^{(\Sigma)^*}$  was then corrected and found to be  $0.91 \pm 0.5$ . The error assumed is somewhat

smaller than our statistical error, since the same value of  $E_{\pi^-}^{(2)*}$  was obtained by the  $K^-$ -Collaboration<sup>1)</sup>, too.

The final emission values used in the present experiment (see section 4) were obtained by a least square fit applied to (1)–(4) above.

### References

- I E. LOHRMANN, M. NIKOLIĆ, M. SCHNEEBERGER, P. WALOSCHEK, and H. WINZELER, *Nuovo Cimento* 7, 163 (1958).
- II Y. EISENBERG, W. KOCH, E. LOHRMANN, M. NIKOLIĆ, M. SCHNEEBERGER, and H. WINZELER, *Nuovo Cimento*, 8, 663 (1958).
- III Y. EISENBERG, W. KOCH, E. LOHRMANN, M. NIKOLIĆ, M. SCHNEEBERGER, and H. WINZELER, *Nuovo Cimento* 9, 745 (1958).
- IV Y. EISENBERG, W. KOCH, M. NIKOLIĆ, M. SCHNEEBERGER, and H. WINZELER, *Nuovo Cimento* 11, 351 (1959).
- V M. NIKOLIĆ, Y. EISENBERG, W. KOCH, M. SCHNEEBERGER, and H. WINZELER, *Helv. Phys. Acta* 3, 221 (1960).
- 1)  $K^-$ -Collaboration, Part. I: *Nuovo Cimento* 13, 690 (1959); Part II: Preprint 1959.
- 2) F. C. GILBERT, CH. E. VIOLET, and R. S. WHITE, *Phys. Rev.* 107, 228 (1957).
- 3) B. A. NIKOL'SKII, L. P. KUDRIN, and S. A. ALI-ZADE, *JEPT (USSR)* 32, 48 Jan. 1957).
- 4) L. W. ALVAREZ, Kiev reports 1959.
- 5) S. C. FREDEN, F. C. GILBERT, and R. S. WHITE, Preprint 1959, UCRL 5629-T.
- 6) R. E. MASHAK, *Meson Physics*.
- 7) P. B. JONES, *Phil. Mag.* 3, 33 (1958), also private communication from Y. EISENBERG, and D. KESSLER.
- 8) G. FERRARI, L. FERRETTI, R. GESSAROLI, E. MANARESI, E. PEDRETTI, G. PUPPI, G. QUARENINI, A. RANZI, A. STANGHETTINI, and S. STANTIC, *Nuovo Cimento Suppl. al. vol. 4*, 914 (1956).
- 9) R. H. MILLER, *Nuovo Cimento* 6, 882 (1957).
- 10) T. B. DAY, G. A. SNOW, and J. SUCHER, *Phys. Rev. Letters* 3, 61 (1959).
- 11) R. H. CAPPS, *Phys. Rev.* 107, 239 (1957).
- 12) Bologna Group: private communication to the  $K^-$ -Collaboration (see (1)).